

AN INTEGRAL CONDITION FOR CORE-COLLAPSE SUPERNOVA EXPLOSIONS

JEREMIAH W. MURPHY¹ AND JOSHUA C. DOLENCE²*Draft version February 25, 2019*

ABSTRACT

We derive an integral condition for core-collapse supernova explosions and use it to construct a new diagnostic of explodability. The fundamental challenge in core-collapse supernova theory is to explain how a stalled accretion shock revives to explode a star. In this manuscript, we assume that shock revival is initiated by the delayed-neutrino mechanism and derive an integral condition for shock expansion, $v_s > 0$. Assuming that $v_s > 0$ corresponds to explosion, we recast this integral condition as a dimensionless condition for explosion, $\Psi > 0$. Using 1D simulations, we confirm that $\Psi = 0$ during the stalled phase and $\Psi > 0$ during explosion. Having validated the integral condition, we use it to derive a useful explosion diagnostic. First, for a given set of parameters, we find the family of solutions to the steady-state equations, parameterized by shock radius R_s , yielding $\Psi(R_s)$. For any particular solution, $\Psi(R_s)$ may be negative, zero, or positive, and, since $\Psi \propto v_s$, this corresponds to a solution with a receding, stationary, or expanding shock, respectively. Within this family, there is always a solution with a minimum Ψ , Ψ_{\min} . When $\Psi_{\min} < 0$, there always exists a stalled accretion shock solution, but when $\Psi_{\min} > 0$, all solutions have $v_s > 0$. Therefore, $\Psi_{\min} = 0$ defines a critical hypersurface for explosion, and we show that the critical neutrino luminosity curve proposed by Burrows & Goshy (1993) is a projection of this more general critical condition. Finally, we propose and verify with 1D simulations that Ψ_{\min} is a reliable and accurate explosion diagnostic.

Subject headings: supernovae: general — hydrodynamics — methods: analytical — methods: numerical — shock waves

1. INTRODUCTION

The question of how typical massive stars explode as core-collapse supernovae (CCSNe) has plagued theorists for decades (Colgate & White 1966). The collapse and bounce of the Fe core of a massive star launches a strong shock wave; however, this prompt shock quickly stalls due to electron capture, nuclear dissociation, and neutrino emission (Hillebrandt & Mueller 1981; Mazurek et al. 1982; Mazurek 1982). Thus the explosive shock is momentarily aborted producing a stalled accretion shock. If the shock remains stalled, the explosion will fail and the proto-neutron star will continue to accrete, eventually collapsing to a black hole (O’Connor & Ott 2011). But we know stars explode and leave neutron stars a large fraction of the time (Fryer et al. 2012). Therefore, the fundamental question in core-collapse theory is how does a CCSN transition from a stalled accretion shock phase into a phase of runaway shock expansion that explodes the star? In this paper, we derive an integral condition that divides stalled-shock solutions from explosive solutions.

The prevailing view is that neutrinos help to reinvigorate the stalled shock, leading to runaway expansion (Bethe & Wilson 1985; Janka 2012; Burrows 2013). A large neutrino flux cools the proto-neutron star and surrounding regions; about half of that luminosity comes from neutrinos diffusing out of the natal proto-neutron star and the rest is emitted directly as accretion luminosity by the accreting stellar material. A fraction of these neutrinos recapture just below the shock, depositing enough energy in the post-shock mantle to reinvigorate

the stalled accretion shock and initiate explosion. However, when this picture is simulated in numerical models with significant (though perhaps not sufficient) detail, the final and most important element — explosion — remains elusive or, at best, inconsistent with observations (Ott et al. 2008; Müller et al. 2012b; Hanke et al. 2013; Takiwaki et al. 2014; Lentz et al. 2015; Dolence et al. 2015). Therefore, a major challenge for simulators has been to understand the various physical effects that influence the unsatisfactory outcomes, all in the context of enormously complicated and expensive simulations. This process of interpretation has inevitably relied on some easily understood models that one hopes encapsulate the important physics of the problem.

In that context, perhaps the most impactful model was proposed by Burrows & Goshy (1993). They proposed that the essence of the core-collapse problem is captured by considering a simple boundary value problem. The inner boundary is set at the proto-neutron star “surface,” defined by a neutrino optical depth of $2/3$, where a temperature and therefore luminosity is specified. The outer boundary is at the stalled shock, where the post shock solutions match the nearly free-falling stellar material upstream via the jump conditions. Burrows & Goshy (1993) proceeded to show that hydrodynamic solutions with a stationary shock only exist below a critical luminosity and accretion rate curve. Above this curve, no stalled shock solutions exist. They speculated that this critical curve, separating stationary from non-stationary solutions, also represents a critical curve for explosion; non-stationary solutions are explosive. Subsequent work with parameterized 1D, 2D, and 3D core-collapse models have confirmed qualitatively that such a critical curve exists (Murphy & Burrows 2008;

¹ Florida State University, jeremiah@physics.fsu.edu² Los Alamos National Laboratory

Hanke et al. 2012; Dolence et al. 2013; Couch 2013), but its precise location in parameter space depends on other details of the problem including, e.g., the structure of the progenitor, hampering the use of the critical curve in practice (Suwa et al. 2014; Dolence et al. 2015).

Nonetheless, the idea of criticality has framed much of the discussion surrounding the simulation results and has motivated the introduction of heuristic and approximate measures of “nearness to explosion.” For example, many have suggested that the ratio of the advection timescale³ to heating timescale⁴ captures an important aspect of the problem, with values $\gtrsim 1$ conducive to explosion (Janka & Keil 1998; Thompson 2000; Thompson et al. 2005; Buras et al. 2006a; Murphy & Burrows 2008). Similarly, Pejcha & Thompson (2012) argue that their “antesonic” condition represents a critical condition for explosion. Both conditions, however, suffer the same afflictions; they lack precise critical values and they both run away only after explosion commences. These shortcomings have led to the practice of measuring these parameters as a function of simulation time and deciding on “critical values” *ex post facto* (Müller et al. 2012b; Dolence et al. 2013; Couch 2013). Clearly, this is unsatisfactory and leads to little more insight than simply identifying explosions with runaway shock radii. In principle, these critical values may even be reached precisely *because* of explosion; the relationship may be symptomatic rather than causal.

In this work, we revisit the idea of criticality, generalizing the critical-curve concept to a critical hypersurface that depends on all of the relevant parameters. We show that for a fixed set of parameters, there is a family of possible solutions. Depending upon the parameters, each family falls into one of two categories. In one category, the family consists of solutions with negative, zero, or positive shock velocity. For such a family, the zero-shock-velocity solution is the quasi-stationary solution. In the second category, all possible solutions have positive shock velocity. These two categories are divided by a critical hypersurface, which may be expressed as a single dimensionless parameter.

This new condition for explosion, the critical hypersurface and associated dimensionless parameter, proves to be a useful diagnostic for core-collapse simulations. For one, we empirically show that the hypersurface corresponds to the transition to explosion in parameterized one dimensional CCSN models. Further, the associated dimensionless parameter reliably and quantitatively indicates when explosions commence. Since we derive the parameter directly from the equations of hydrodynamics, its usefulness is not limited by the ad hoc calibrations of other popular measures. Finally, when combined with semi-analytic models, we show that our single parameter yields an accurate and reliable measure of nearness to explosion.

For your convenience, the structure of this manuscript is as follows. In section 2, we review the boundary value problem that describes the core-collapse problem (Burrows & Goshy 1993) and identify the important parameters of the problem. With this framework, and the

proposition that $v_s > 0$ corresponds to explosion, we derive the integral condition for explosion in section 3. Then in section 4, we validate the integral conditions for explosion with 1D parameterized simulations. In section 5, we use the integral condition to investigate the family of steady-state solutions and propose an explosion diagnostic. Then in section 6, we compare the reliability of the integral condition explosion diagnostic with other popular explosion measures, finding that the integral condition outperforms them all. Finally, for a brief summary of the conclusions, cautionary notes, and future prospects, see section 7.

2. QUASI-STEADY SOLUTIONS: A BOUNDARY VALUE PROBLEM

The fundamental question of core-collapse theory is how does the stalled accretion shock phase transition into a dynamic explosion? In other words, what are the conditions for which the shock velocity, v_s , is persistently greater than zero? While the shock is stationary, the steady-state assumption is quite good. Under this assumption, the entire region below the shock may be treated as a boundary value problem (Burrows & Goshy 1993). The upper boundary is set by the properties of the nearly free falling stellar material and the jump conditions at the shock, while the lower boundary is the surface of the neutron star. Later, we derive a condition in which there are no more $v_s = 0$ solutions, and the only solutions left are those in which $v_s > 0$. To understand when the steady-state solutions are no longer viable, we first must understand the stalled accretion shock solution and the important parameters of the problem.

To begin, the governing conservation equations are

$$\frac{\partial \rho}{\partial t} + \nabla \cdot (\rho \mathbf{v}) = 0, \quad (1)$$

$$\frac{\partial (\rho \mathbf{v})}{\partial t} + \nabla \cdot (\rho \mathbf{v} \mathbf{v}) + \nabla P = \rho \nabla \phi, \quad (2)$$

and

$$\frac{\partial (\rho E)}{\partial t} + \nabla \cdot \left[\rho \mathbf{v} \left(h + \frac{v^2}{2} \right) \right] = \rho \mathbf{v} \cdot \nabla \phi + \rho q, \quad (3)$$

where ρ is the mass density, \mathbf{v} is the velocity, P is the pressure, ϕ is the gravitational potential, $E = \varepsilon + v^2/2$ is the internal plus kinetic specific energy, and $h = \varepsilon + P/\rho$ is the specific enthalpy. In this paper, we approximate the heating and cooling, q as

$$q = \frac{L_\nu \kappa}{4\pi r^2} - C \left(\frac{T}{T_0} \right)^6. \quad (4)$$

The first term is a model in which we treat the neutrino heating as if all neutrinos are emitted from the proto-neutron star “surface” with a luminosity of L_ν (Janka 2001; Murphy & Burrows 2008; Murphy et al. 2013). κ is the opacity for absorbing neutrinos in the region above the “surface”, which is proportional to T_ν^2 . In this paper, the surface of the proto-neutron star is given by $\tau = \int_{R_{NS}}^\infty \kappa \rho dr = 2/3$, which implicitly defines the proto-neutron star radius (R_{NS}) as the neutrinospheric radius. In practice, we find that this corresponds to a density of $\rho_{NS} \approx 7 \times 10^{10}$ g/cc. The second term is the neutrino cooling due to thermal weak interactions (Janka 2001).

³ time to advect through the net heating region

⁴ time to significantly change the thermal energy in the net heating region

In a quasi-steady state, the time-derivative terms are small and the problem is well-approximated by setting these terms to zero. The solution to the resulting boundary value problem describes the conditions of the flow between the proto-neutron star surface and the bounding stalled shock in terms of the important parameters of the problem: L_ν , T_ν , R_{NS} , M_{NS} (proto-neutron star mass), and \dot{M} (accretion rate). See Figure 1 for a schematic of the boundary value problem and the most important parameters of the problem.

3. DERIVING AN INTEGRAL CONDITION FOR $V_S > 0$

We reduce the core-collapse problem to a set of integral conditions and show that this leads to a critical condition for explosions. Before we derive the integral conditions, let us motivate why we consider the integral equations at all. Usually, the governing equations (eqs. 1-3) are presented in differential form, but one could just as easily present them in integral form. The two forms represent exactly the same information. One's choice is determined by the ease and method for finding solutions. For example, it is typically easier to work with the differential form when one needs to find numerical solutions, but if one seeks an analytic solution, the integral equations can be easier to use. For example, in finding the motion of a body in a potential field, one may solve the equations of motion, or one may use the integral condition, conservation of energy.

We argue that the integral equations provide an easier route to deriving a unified condition for explosions. Because the shock is a crucial component of the core-collapse problem, when we derive the explosion condition we embark in a route that is similar to deriving the Rankine-Hugoniot shock jump conditions. The route to deriving these jump conditions involves using the integral equations in the context of a moving boundary, the shock.

3.1. The generic integral condition

As in deriving the Rankine-Hugoniot conditions, we start with the conservation equations and the Reynolds Transport theorem. Consider a generic conserved quantity, q , which could represent a mass density, momentum density, energy density, etc. Generically, one may define the total conserved quantity in region $D(t)$ as $\int_{D(t)} q dV$ and the time-rate-of-change of this conserved quantity is $\frac{d}{dt} \left(\int_{D(t)} q dV \right)$. The Reynolds Transport theorem decomposes this time-rate-of-change into an Eulerian component and a component that accounts for the motion of the boundaries of region $D(t)$:

$$\frac{d}{dt} \left(\int_{D(t)} q dV \right) = \int_{D(t)} \frac{\partial q}{\partial t} dV + \oint_{\partial D(t)} q \mathbf{v}_b \cdot d\mathbf{S}, \quad (5)$$

with $\partial D(t)$ the surface of this domain, $d\mathbf{S}$ the surface element, and \mathbf{v}_b the velocity of the surface. To make use of the Reynolds Transport theorem, we need an expression for the Eulerian time derivative, $\partial q / \partial t$. The conservation equation provides such an expression. A general conservation equation has the following form

$$\frac{\partial q}{\partial t} + \nabla \cdot \mathbf{f} = s, \quad (6)$$

where \mathbf{f} is the flux of q , and s is a source/sink of q . With these two equations (eqs. 5 & 6) we may now proceed to derive the integral conditions.

To construct the appropriate boundary value problem, we must choose the appropriate boundaries. We consider a boundary value problem where the lower boundary is at r_1 and the upper boundary is at r_2 . The overall problem is divided into two domains, with a different solution in each domain. The pre-shock solution is in the domain $(r_s(t), r_2]$, the post-shock solution is in the domain $[r_1, r_s(t))$, and the two solutions are joined by the Rankine Hugoniot jump conditions at $r_s(t)$. With the boundaries defined, we now define the integral equations.

First, we integrate eq. (6) from r_1 to r_2 , and since the boundaries are constant in time, we have

$$\frac{d}{dt} \left(\int_{r_1}^{r_2} q dV \right) = \int_{r_1}^{r_2} \frac{\partial q}{\partial t} dV = \int_{r_1}^{r_2} (-\nabla \cdot \mathbf{f} + s) dV. \quad (7)$$

Next, we rewrite the left hand side of eq. (7) to explicitly express the shock radius. In order to do this, we must divide the integral into two regions, above and below the shock, and we use the Reynolds Transport equation (eq. 5). This gives

$$\begin{aligned} \frac{d}{dt} \left(\int_{r_1}^{r_2} q dV \right) &= v_s 4\pi r_s^2 (q_{s-\epsilon} - q_{s+\epsilon}) \\ &+ \int_{r_1}^{r_s(t)} \frac{\partial q}{\partial t} dV + \int_{r_s(t)}^{r_2} \frac{\partial q}{\partial t} dV. \end{aligned} \quad (8)$$

In the core-collapse problem, the pre-shock solution is nearly in free-fall and can be solved analytically. Therefore, the problem reduces to finding the post-shock solution subject to the lower boundary, the surface of the NS, and the upper boundary, the shock. Now, we take the limit that r_2 approaches $r_s(t)$. In this limit, we have the following simplifications

$$\lim_{r_2 \rightarrow r_s(t)} q_{s+\epsilon} = q_2 \text{ and } \lim_{r_2 \rightarrow r_s(t)} \int_{r_s(t)}^{r_2} \frac{\partial q}{\partial t} dV = 0, \quad (9)$$

which, when inserted into eq. (8), results in the simpler integral equation:

$$\frac{d}{dt} \left(\int_{r_1}^{r_2} q dV \right) = v_s 4\pi r_s^2 (q_{s-\epsilon} - q_2) + \int_{r_1}^{r_s(t)} \frac{\partial q}{\partial t} dV. \quad (10)$$

By plugging eq. (10) into eq. (7), we arrive at the general integral equation

$$v_s 4\pi r_s^2 (q_{s-\epsilon} - q_2) + \int_{r_1}^{r_s(t)} \frac{\partial q}{\partial t} dV = 4\pi (f_1 r_1^2 - f_2 r_2^2) + \int_{r_1}^{r_2} s dV. \quad (11)$$

Note that if we take the limit that r_1 approaches r_s from below, this reduces to the shock jump conditions, but if we retain r_1 at the neutron star surface, we have the general integral equations describing the post shock structure. If we assume steady-state, then this reduces to

$$v_s 4\pi r_s^2 (q_{s-\epsilon} - q_2) = 4\pi (f_1 r_1^2 - f_2 r_2^2) + \int_{r_1}^{r_2} s dV. \quad (12)$$

Finally, if we assume that explosion occurs when $v_s \geq 0$,

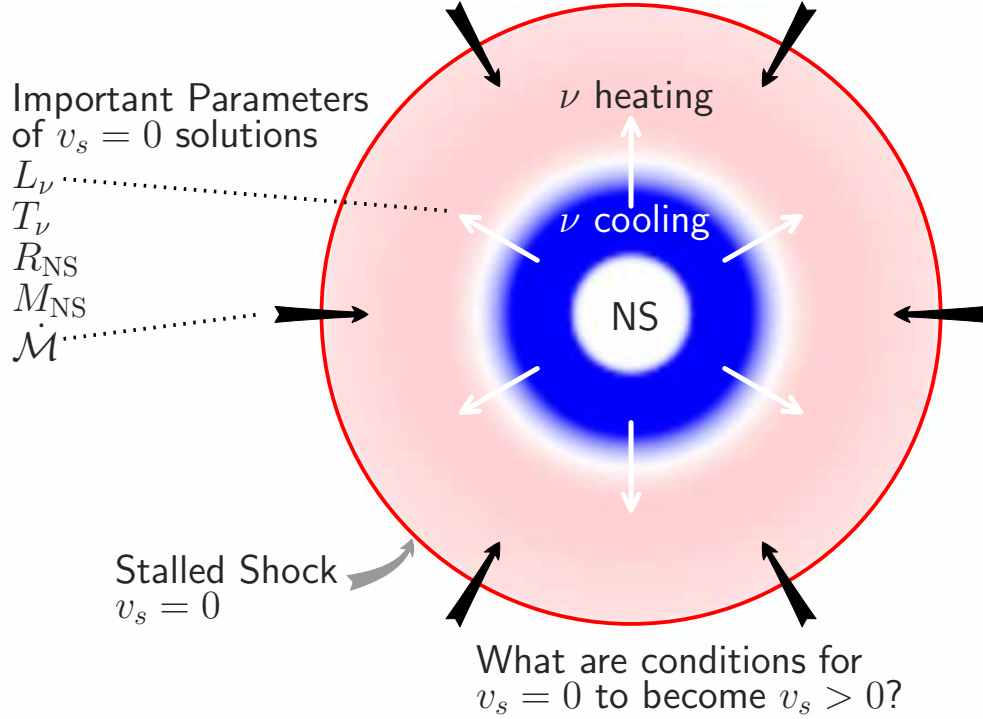


Figure 1. After the bounce shock stalls, the post-shock flow settles into a quasi-steady configuration. The solutions satisfy a boundary value problem between the neutron star “surface” and the stalled shock. The important parameters in determining the steady-state solutions are the neutrino luminosity being emitted from the core (L_ν), the temperature of the neutrinos (T_ν), the mass accretion rate onto the shock and NS (\dot{M}), the NS radius (R_{NS}), and the NS mass (M_{NS}). The fundamental challenge in core-collapse theory is to understand how $v_s = 0$ transitions to $v_s > 0$. In section 3, we derive such a condition.

then the generic integral condition for explosion becomes

$$4\pi(f_1 r_1^2 - f_2 r_2^2) + \int_{r_1}^{r_2} s dV \geq 0. \quad (13)$$

3.2. Integral Conditions Using Momentum and Energy Equations

Next, we use the momentum equation (2) and energy equation (3) to suggest dimensionless integral conditions for explosion. Substituting the corresponding fluxes and source terms for the momentum and energy equations into the generic integral condition, eq. (13), leads to two integral conditions

$$(P_1 + \rho_1 v_1^2) r_1^2 - (P_2 + \rho_2 v_2^2) r_2^2 + \int_{r_1}^{r_2} 2Pr dr - \int GM\rho dr \geq 0, \quad (14)$$

and

$$\dot{M} \left(h_1 + \frac{v_1^2}{2} - \phi_1 - h_2 - \frac{v_2^2}{2} + \phi_2 \right) + \int_{r_1}^{r_2} \rho q dV \geq 0. \quad (15)$$

In the context of the core-collapse problem, we can further simplify these integral conditions. First, let's set the inner boundary to the surface of the neutron star $r_1 = R_{\text{NS}}$, and the outer boundary is the shock position, $r_2 = R_s$. Second, the material accreting onto the shock has a Bernoulli parameter of approximately zero, $h_2 + v_s^2/2 - \phi_2 \approx 0$. Third, the mass, M , is dominated by the neutron star mass, M_{NS} . Fourth, the kinetic energy at the neutron star surface is much less than the enthalpy

or gravitational potential, $v_1^2 \ll h_1 \sim P_1/\rho_1 \sim \phi_1$. Fifth, the pre-shock enthalpy and pressure are much smaller than the pre-shock kinetic energy. Under these assumptions, the conditions for $v_s > 0$ become

$$y_1 - 2z_2 x_s + \int_1^{x_s} (2y - 1)z dx \geq 0, \quad (16)$$

and

$$\Sigma \equiv \frac{\dot{Q}}{\dot{M}\phi_{\text{NS}}} + 1 - \left(\frac{h}{\phi} \right)_{\text{NS}} \geq 0, \quad (17)$$

where $y = P/\rho/\phi$, $z = \rho/\rho_1$, $x = r/R_{\text{NS}}$, $\dot{M} = -\dot{M}$, and $\dot{Q} = \int_{R_{\text{NS}}}^{R_s} \rho q dV$. We rewrite the momentum condition as

$$\Psi \equiv \frac{y_1}{\eta} - \frac{2z_2 x_s}{\eta} + \frac{2 \int yz dx}{\eta} - 1 \geq 0, \quad (18)$$

where $\eta = \int z dx$. Finally, we have our integral conditions for explosion: $\Psi \geq 0$ (eq. 18) is derived from the momentum equation, and $\Sigma \geq 0$ (eq. 17) is derived from the energy equation.

4. VALIDATING $\Psi \geq 0$ AND $\Sigma \geq 0$ WITH 1D PARAMETERIZED SIMULATIONS

Later, we use Ψ to propose an explosion diagnostic for core-collapse simulations, but first we verify in this section that $\Psi = 0$ and $\Sigma = 0$ during the stalled shock phase and that $\Psi > 0$ and $\Sigma > 0$ during explosion. To perform these validating tests, we calculate Ψ and Σ in 1D parameterized simulations.

The 1D simulations are calculated using a new code **Cufe**, which will be described fully in Murphy & Bloor (in prep. 2015). **Cufe** solves the equations of hydrodynamics eqs. (1-3) using higher-order Godunov techniques. The grid is logically Cartesian but employs a generalized metric allowing for a variety of mesh geometries. For this study, we use spherical coordinates. The progenitor model is the $12 M_{\odot}$ model of Woosley & Heger (2007), the equation of state (EOS) includes effects of dense nucleons around and above nuclear densities, nuclear statistical equilibrium, electrons, positrons, and photons (Hempel et al. 2012). For the neutrino heating and cooling we use the approximate local descriptions of Janka (2001) and Murphy et al. (2013).

Recall that there are five important parameters that describe the steady-state accretion solutions: L_{ν} , T_{ν} , M_{NS} , R_{NS} , and \dot{M} . Two of these, L_{ν} and T_{ν} , we set in the parameterized simulations; the rest we calculate self-consistently given the equations of hydrodynamics, the progenitor structure, and the equation of state. The top panel of Figure 2 shows the time evolution of M_{NS} , R_{NS} , and \dot{M} ; we highlight the post-bounce phase of a model that does not explode. \dot{M} starts quite high, well above $1 M_{\odot}/\text{s}$, but then drops down to $\sim 0.2 M_{\odot}/\text{s}$ near the end of the simulation. At around 500 ms after bounce \dot{M} has a significant drop, which is a result of a density shelf advecting through the shock. Throughout this paper, you will notice that this significant drop in \dot{M} gets imprinted on many of the explosion diagnostics, including the shock radius vs. time in the bottom panel of Figure 2.

To sample a range of explosion timescales, we vary the light bulb neutrino luminosity, L_{ν} . The bottom panel of Figure 2 shows the resulting shock radii vs. time labeled by L_{ν} in units of 10^{52} erg/s. In all models, the shock forms at 153 ms after the start of the simulations and quickly stalls between ~ 150 to ~ 200 km. The general trend is that the higher luminosity models explode earlier than lower luminosity models. The lowest luminosity model does not explode at all. However, it does experience a significant outward adjustment and oscillation of the shock as \dot{M} drops significantly around 500 ms after bounce. The $L_{\nu} = 2.5$ & 3.0 models explode during the advection of the density shelf. An obvious feature present in the shock radius evolution plot are the shock radius oscillations. They are often present in 1D simulations near explosion (Ohnishi et al. 2006; Buras et al. 2006b; Murphy & Burrows 2008), and Fernández (2012) suggests that they might be related to the advective-acoustic feedback loop that is responsible for the SASI in multi-D simulations.

For each of the models, we calculate Ψ and Σ directly from the simulations; see Figures 3 & 4 for the results. Ψ is indeed zero during the steady-state phase and $\Psi > 0$ during explosion. Note, however, Ψ never achieves a value greater than about 0.02. This indicates how subtle the core-collapse problem is; even during the strongest explosion, the profile deviates from hydrostatic equilibrium only by about 2%. Regardless, the fact that simulations roughly validate $\Psi \geq 0$ implies that Ψ is a good dimensionless explosion diagnostic. Qualitatively, Σ is also roughly zero during the steady-accretion phase and greater than 0 during explosion. However, the os-

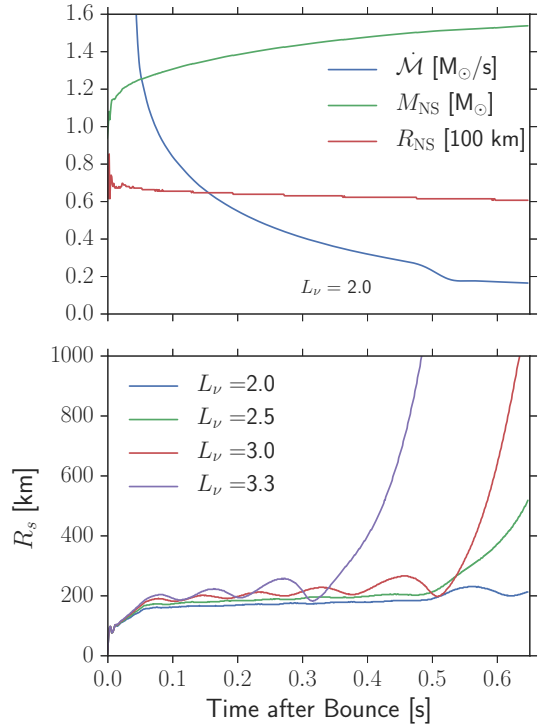


Figure 2. Characteristics of 1D parameterized simulations. **Top panel:** Mass accretion rate (\dot{M}), mass of neutron star (M_{NS}), and radius of neutron star (R_{NS}) vs. time for the lowest luminosity simulation. Later we compare the integral condition for explosion with parameterized simulations. Here, we show the three important parameters of the steady-state problem highlighted in Figure 1, which are calculated self-consistently in the simulations. The evolution of these parameters with time is similar for all simulations, so we just show the lowest luminosity simulation here. **Bottom panel:** Shock radius (R_s) vs. time for four 1D parameterized simulations. To facilitate comparison with the integral condition, we parameterize the neutrino heating and cooling. The neutrino luminosities are in units of 10^{52} erg/s.

oscillations of the shock are much more apparent in the behavior of Σ compared to Ψ . Therefore, we conclude that Ψ is practically a better condition for explosion.

5. Ψ_{min} : A NEARNESS-TO-EXPLOSION CONDITION

The fact that $\Psi > 0$ during explosion (Figure 3) suggests that Ψ has the potential to be a good explosion diagnostic. However, just calculating Ψ from the simulations is not the most useful condition; Ψ remains zero during the non-exploding phase and it only deviates from zero while the simulation is exploding. That behavior is not a very useful explosion diagnostic, and one might as well just use the shock radius. In fact, most explosion “conditions” or “diagnostics” to date have this problem. They do not provide a nearness-to-explosion condition. What we need is a way to translate the $\Psi \geq 0$ condition into a useful nearness-to-explosion condition. Fortunately, Ψ lends itself to such an explosion diagnostic.

Our strategy for developing a nearness-to-explosion condition is to extract L_{ν} , T_{ν} , R_{NS} , M_{NS} , and \dot{M} from the simulations and calculate the steady-state solutions for each set of parameters. For a given set of parameters, there is a family of solutions to the steady-state equations, each with a different shock radius⁵. Each so-

⁵ Far from the equilibrium shock radius, these solutions are likely

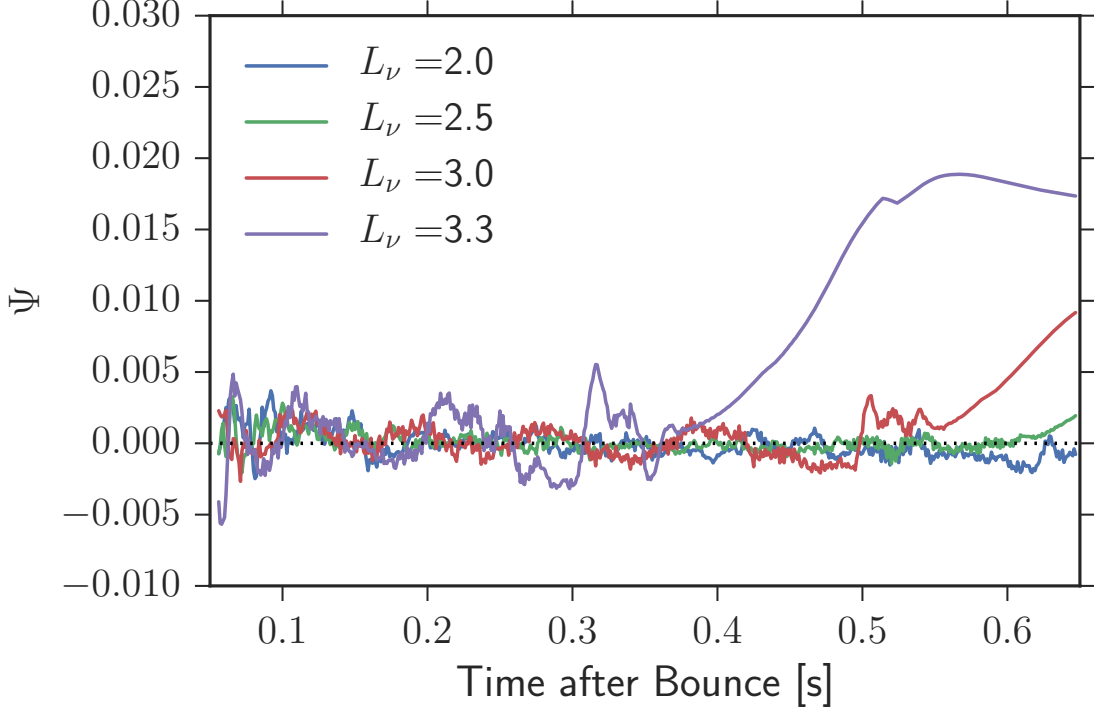


Figure 3. Ψ , the explosion condition, evaluated from the 1D simulations as a function of time. In section 3, we derive an integral condition for explosion based upon the momentum equation; we derive that $v_s \geq 0$ corresponds to $\Psi \geq 0$. To test whether this condition corresponds to explosion, we evaluate Ψ for the 1D parameterized simulations described in section 4; we find that $\Psi = 0$ during the stalled-shock phase, and $\Psi > 0$ during explosion. These results strongly suggest that $\Psi \geq 0$ is a useful condition for explosion. However, this condition does not by itself predict explosion. It only indicates that explosion has occurred. In section 5, we propose a method to turn $\Psi \geq 0$ into a useful explosion diagnostic.

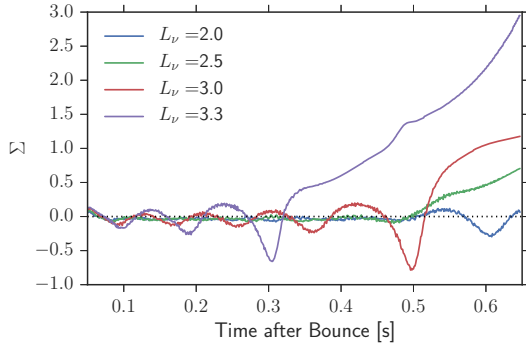


Figure 4. Σ , the explosion condition, evaluated from the 1D simulations as a function of time. $\Sigma \geq 0$ is the condition based upon the energy equation. Like Ψ (see Figure 3), Σ is about zero during the stalled phase and greater than zero during explosion. Unlike Ψ , Σ seems to be more susceptible to shock oscillations. Therefore, in section 5, when we propose an explosion diagnostic, we use the $\Psi \geq 0$ condition.

lution has a value for Ψ which may be < 0 , $= 0$, or > 0 , which correspond to solutions with $v_s < 0$, $v_s = 0$, or $v_s > 0$, respectively. The $v_s = 0$ ($\Psi = 0$) solution is a quasi-equilibrium solution. We will show that for each family of solutions, there is always a minimum Ψ , which we denote Ψ_{\min} . When $\Psi_{\min} < 0$, then $v_s = 0$ solutions

incorrect in detail since they correspond to situations that are far from a steady-state. However, our approach does not require accurate models far from equilibrium

exists. However, when $\Psi_{\min} > 0$, the only solutions that exist have $v_s > 0$. Therefore, we propose that Ψ_{\min} is an excellent explosion diagnostic providing a nearness-to-explosion condition. Figures 5 & 6 illustrate these points.

Having outlined the strategy, we now provide the specifics in calculating Ψ_{\min} . We begin with the steady-state equations

$$\dot{M} = 4\pi r^2 \rho v, \quad (19)$$

$$\rho \frac{dv}{dr} + \frac{dP}{dr} = -\rho \frac{\phi}{r} \quad (20)$$

and

$$\frac{\dot{M}}{4\pi r^2} \frac{d\varepsilon}{dr} + P \frac{d(r^2 v)}{r^2 dr} = \rho q. \quad (21)$$

To solve these equations, we need an equation of state to relate P in terms of ε and ρ , and we need boundary conditions. For the region that we consider, above the neutrinosphere and below the shock, the dominant contributors to the EOS are neutrons, protons, helium nuclei (α), positrons, electrons, and photons. We treat the neutrons, protons, and α s as an ideal non-relativistic gas; the positrons, electrons, and photons constitute the relativistic part of the plasma, and we consider the positrons and electrons in an arbitrary degeneracy. To calculate the relative abundances of neutrons, protons, and α s, we assume nuclear statistical equilibrium for these three components and use the Saha equation to calculate their

abundances. See appendix B for the details in calculating the EOS and the abundances.

In the spirit of Burrows & Goshy (1993) and others (Yamasaki & Yamada 2005, 2006; Yamasaki & Foglizzo 2008), we solve the steady-state equations, Eqs. (19-21), using the Rankine-Hugoniot jump conditions for a stalled shock. The jump conditions give the post-shock state (subscript s) in terms of the pre-shock state (subscript 2):

$$\rho_s v_s = \rho_2 v_2, \quad (22)$$

$$\rho_s v_s^2 + P_s = \rho_2 v_2^2 + P_2, \quad (23)$$

and

$$h_s + \frac{v_s^2}{2} = h_2 + \frac{v_2^2}{2}. \quad (24)$$

For the pre-shock state, we make the following assumptions that enable analytic solutions of the conditions. First, we assume that $\dot{M} = 4\pi r_s^2 \rho_2 v_2$ is a constant. Second, we assume that the star is accreting onto the shock at a large fraction of free fall, so the pre-shock speed is given by $v_2^2 = 2\alpha_v \phi(R_s)$. Third, we assume that the pre-shock Bernoulli constant is roughly zero, $h_2 + v_2^2 - \phi(R_s) \approx 0$. Finally, we assume a gamma-law relationship for the pre-shock pressure, internal energy, and density: $\gamma_4 \equiv P/(\rho\varepsilon) + 1$. Under these assumptions, the pre-shock pressure is

$$P_2 = \frac{\gamma_4 \rho_2 (1 - \alpha_v)}{\gamma_4 - 1} \phi(R_s). \quad (25)$$

Specifying \dot{M} , α_v , γ_4 , and R_s then sets the boundary conditions at the shock. When Burrows & Goshy (1993) first introduced the critical luminosity, they specified one more boundary condition at the base: $\tau = \int \kappa \rho dr = 2/3$. This extra condition enables one to self-consistently solve for the shock radius that permits a steady-state-stalled-shock solution. Yamasaki & Yamada (2005) noted that the density at the radius where $\tau = 2/3$ is almost always the same, so one can easily replace the τ condition by specifying a specific density at the neutrinosphere, or neutron star surface. We take a slightly different approach in this paper.

First of all, we use the 1D simulations to inform the values for \dot{M} , M_{NS} , R_{NS} , α_v , and γ_4 , and of course, we set L_ν and T_ν to the values used for the 1D parameterized simulations. Then we find solutions to the steady-state equations for a wide range of shock radii. These solutions represent a family of solutions at different R_s but all with the same parameters. For each solution and associated R_s , we evaluate Ψ , where we follow Yamasaki & Yamada (2005) and set $\rho_1 = 7 \times 10^{10}$ g/cc. Since Ψ is proportional to the shock velocity, Ψ naturally shows which solutions have $v_s < 0$, $v_s = 0$, or $v_s > 0$. The $v_s = 0$ solution corresponds to the steady-state-stalled-shock solution.

Figure 5 shows the outcome of this process. Each line corresponds to a specific set of parameters and one family of solutions. For clarity, we only vary L_ν between different families of solutions. For low values of L_ν , all three solutions ($v_s > 0$, $v_s = 0$, and $v_s < 0$) are possible. For low R_s , $\Psi > 0$ implying that $v_s > 0$ and the shock would move outward. For larger R_s , $\Psi < 0$ so $v_s < 0$ and the shock would tend to move inward. In between, at a very specific shock radius, there is a solution which

has $\Psi = 0$ and $v_s = 0$. This solution represents an equilibrium solution. While solutions far from equilibrium are not steady and therefore are poorly represented by the steady-state equations, our approach does not rely on the quantitative accuracy of this representation. For a visual aide of these concepts see Figure 6.

Note that for large values of L_ν there are no solutions for which $\Psi_{\text{min}} < 0$. In those cases, all solutions correspond to $v_s > 0$. There is a very specific set of parameters for which $\Psi_{\text{min}} = 0$. The locus of such parameters defines a critical hypersurface that generalizes but encompasses the critical neutrino luminosity condition of Burrows & Goshy (1993) (see Section 6 for more on this).

To validate that Ψ_{min} satisfies the desired qualities of an explosion diagnostic, we plot Ψ_{min} in Figure 7 for the 1D parameterized simulations. The parameter that we set by hand in each simulation is L_ν and T_ν ; we keep T_ν set at 4 MeV, and vary L_ν . At each time, we extract the other important parameters M_{NS} , R_{NS} , and \dot{M} , which are calculated self-consistently in the simulation. We then calculate the family of steady-state solutions for that set of parameters and find the value of Ψ_{min} . Figure 7 shows that Ψ_{min} has the desired qualities of an explosion condition. Before explosion $\Psi_{\text{min}} < 0$ and during explosion $\Psi_{\text{min}} > 0$. Moreover, we suggest that the value of Ψ_{min} before explosion provides a useful metric for how far away the simulation is from explosion.

6. COMPARISON WITH OTHER EXPLOSION CONDITIONS

In this section, we quickly compare the integral explosion diagnostic, $\Psi_{\text{min}} > 0$ with three other conditions: the critical neutrino luminosity condition (Burrows & Goshy 1993), a timescale ratio condition (Janka & Keil 1998; Thompson 2000; Thompson et al. 2005; Buras et al. 2006a; Murphy & Burrows 2008), and the antesononic condition (Pejcha & Thompson 2012). In this manuscript, we mostly compare the effectiveness of these conditions with the integral condition; in a forthcoming paper (Murphy & Dolence in prep. 2015), we show that one can actually derive all three conditions from the integral condition by making various further approximations. For now, we simply compare the conditions.

Of these three, the most closely related condition is the critical luminosity condition of Burrows & Goshy (1993). In fact, a primary motivation in deriving the integral condition is to derive a condition that shows that the solutions above the critical neutrino luminosity curve correspond to $v_s > 0$. In section 3, we derived the integral condition for $v_s > 0$, and now, in Figure 8, we show that this same integral condition reproduces the critical neutrino luminosity curve of Burrows & Goshy (1993).

To reproduce the critical neutrino luminosity curve in Figure 8, we first fix three of the five important parameters of the problem, R_{NS} , M_{NS} , and T_ν . In other words, we restrict the dimensionality of the integral condition to the L_ν - \dot{M} plane. Then we find the solutions to the steady-state equations (eqs. 19-21) and select the solutions in the L_ν - \dot{M} plane that have $\Psi_{\text{min}} = 0$. The locus of these specific solutions form the solid curve that we show in Figure 8. Above this curve, $\Psi_{\text{min}} > 0$ and therefore all solutions have $v_s > 0$. Below this curve $\Psi_{\text{min}} < 0$,

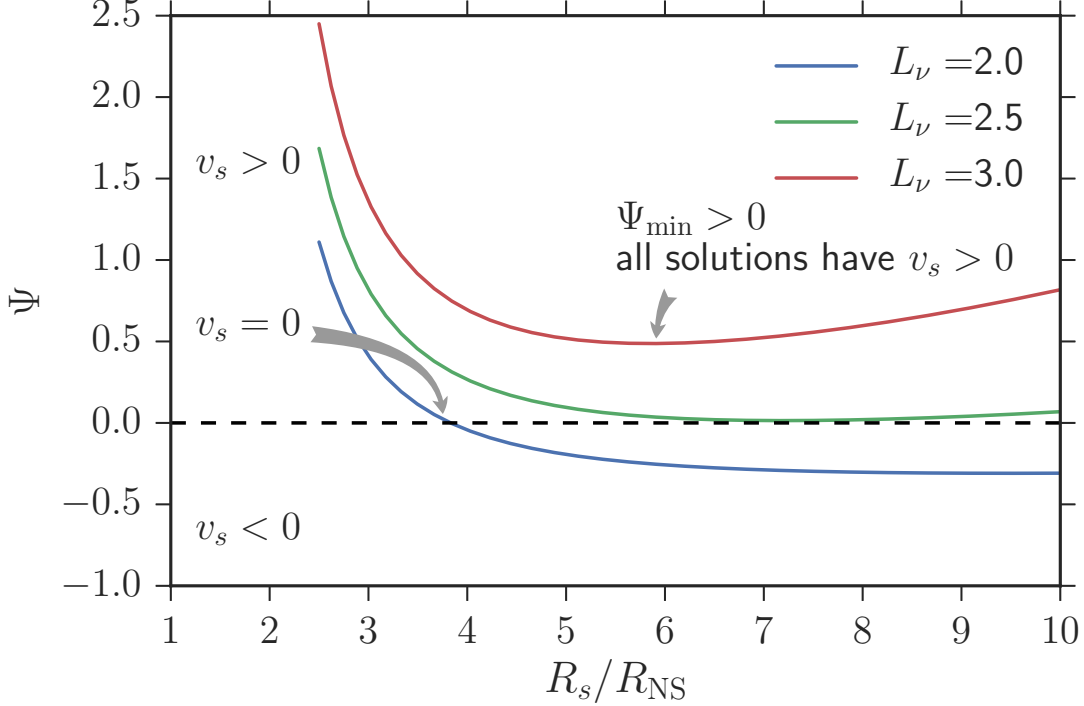


Figure 5. The family of steady-state solutions represented by their values of $\Psi(R_s/R_{\text{NS}})$ for three different neutrino luminosities but all else being equal. For some parameters, Ψ may be negative, zero, or positive. The solution with $\Psi = 0$ ($v_s = 0$) corresponds to the equilibrium solution. For each family, there is a solution with a minimum Ψ , which we denote Ψ_{min} . When $\Psi_{\text{min}} < 0$, a stalled shock ($v_s = 0$) solutions exists, but when $\Psi_{\text{min}} > 0$, only solutions with $v_s > 0$ exist. We propose that $\Psi_{\text{min}} > 0$ is an excellent explosion diagnostic (see Figure 7).

and therefore a steady-state stalled shock solution exists. This curve is exactly the same critical neutrino luminosity curve that Burrows & Goshy (1993) and others have derived. The difference is in the way that it is derived. Burrows & Goshy (1993) solved the steady-state equations looking for solutions for which the shock and $\tau = 2/3$ conditions are satisfied. There is no statement about the behavior of v_s above the curve. Rather than highlighting τ , we instead use the $\Psi_{\text{min}} = 0$ condition, so one readily sees that $v_s > 0$ above the curve.

Besides showing that $v_s > 0$ above the critical neutrino luminosity curve, we also show that $\Psi_{\text{min}} > 0$ is a more general explosion condition than the critical neutrino luminosity. In fact, in the important parameters, $\Psi_{\text{min}} = 0$ represents a critical hypersurface, and the critical neutrino luminosity curve is a projection of this more general critical condition. Remarkably, this critical hypersurface is represented by one dimensionless condition $\Psi_{\text{min}} > 0$.

Another common class of explosion metrics are the timescale ratios in which one compares an advection timescale (τ_{adv}) to a heating timescale (τ_{heat}). Roughly, neutrino heating might be expected to significantly modify the internal energy of the accreting material only when $\tau_{\text{heat}} \lesssim \tau_{\text{adv}}$. Based on this, many have used the ratio $\tau_{\text{adv}}/\tau_{\text{heat}}$ as a diagnostic to indicate how close a model is to explosion for a given snapshot (Janka & Keil 1998; Thompson 2000; Thompson et al. 2005; Buras et al. 2006a; Murphy & Burrows 2008). While this may seem sensible at face value, the timescale

ratio arguments all neglect important aspects of the CCSN problem — cooling, for example. Meanwhile, Murphy & Burrows (2008) and Dolence et al. (2013) have shown that the turbulent dynamics of multi-D lead to longer advection times on average, speculating that this may be an important effect vis-à-vis 1D vs. multi-D.

There are many approximate definitions of τ_{adv} and τ_{heat} (Janka & Keil 1998; Murphy & Burrows 2008; Fernández 2012). Early definitions of the advection time include $\tau_{\text{adv}} = \int_{r_{\text{gain}}}^{r_{\text{shock}}} dr/v_r$, but the most recent definitions use the mass in the gain region and the mass accretion rate

$$\tau_{\text{adv}} = \frac{M_{\text{gain}}}{\dot{\mathcal{M}}}. \quad (26)$$

For the rest of this paper, we adopt this most recent definition. For the heating timescale, the generic approach is to compare a total energy with an integrated heating rate $\tau_{\text{heat}} = E/Q$. Generically, many define the heating rate as $Q = \int_{\text{gain}} (H - C)\rho dV$. The total energy has several definitions, and since none are derived from a firm explosion condition, all are arbitrary. We highlight and use one condition; we consider the total internal energy in the gain region $E = \int_{\text{gain}} \epsilon \rho dV$. Both the choice for the energy scale and the region are completely arbitrary and not derived from an actual explosion condition. In a forthcoming paper (Murphy & Dolence in prep. 2015), we will derive a timescale ratio condition from the integral condition, but for now we just compare to the

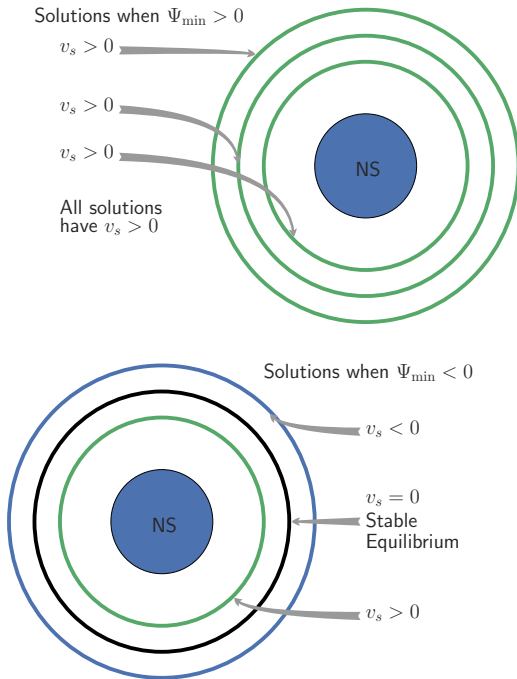


Figure 6. This is an illustration to demonstrate the two regimes seen in Figure 5. If $\Psi_{\min} < 0$, then there are solutions with $v_s < 0$, $v_s = 0$, and $v_s > 0$. In general, the solution with $v_s = 0$ is an equilibrium solution and, as long as it exists, simulations (and presumably Nature) settle on this steady-state stalled shock solution. When $\Psi_{\min} > 0$, the only solutions are ones in which $v_s > 0$. Therefore, Ψ_{\min} seems to be a natural condition for explosion.

arbitrary definitions from the past. For example, the integral energy explosion condition that we derive in section 3 (eq. 17) highlights that it is the Bernoulli parameter that is important and that one should consider the entire region between the neutrino sphere and the shock. Traditionally neither of these have been considered. Instead, one often guessed at a typical energy scale and a region that is important. So we pick one example, the total internal energy in the gain region.

$$\tau_{\text{heat}} = \frac{E_{\text{int}}}{Q}, \quad (27)$$

Figure 9 compares our derived integral condition, Ψ_{\min} , with the approximate timescale ratio condition, $\tau_{\text{adv}}/\tau_{\text{heat}}$. As one might expect, the rough heuristic condition does not perform as well at predicting explosions. Indeed, $\tau_{\text{adv}}/\tau_{\text{heat}}$ is $\mathcal{O}(1)$ before explosion and increases dramatically after explosion. However, the ratio has serious problems as an explosion metric. For example, one might be tempted to conclude that the sharp upward trend in this ratio would be a good indicator of explosion. However, careful inspection of $\tau_{\text{adv}}/\tau_{\text{heat}}$ and the shock radii in Figure 9 shows that $\tau_{\text{adv}}/\tau_{\text{heat}}$ just follows R_s . Therefore, using $\tau_{\text{adv}}/\tau_{\text{heat}}$ is not much more useful than R_s . One might be tempted to use the simulations to calibrate a “critical” value for $\tau_{\text{adv}}/\tau_{\text{heat}}$. However, the results in the literature as well as those shown here indicate that no such “critical” value exists (Müller et al. 2012b; Hanke et al. 2012; Dolence et al. 2013). Simple comparison between the definition of $\tau_{\text{adv}}/\tau_{\text{heat}}$ (eqs. 26 & 27) and the integral conditions (eqs. 17 & 18) shows that

much is missing from the $\tau_{\text{adv}}/\tau_{\text{heat}}$ condition, so its shortcomings should be unsurprising.

The final comparison is between Ψ_{\min} and the antesononic condition of Pejcha & Thompson (2012); see Figure 10. Similar to our motivation, Pejcha & Thompson (2012) were motivated to explain the origin of the critical luminosity curve and possibly derive a more generic condition. They took a slightly different tack. Pejcha & Thompson (2012) considered the family of accretion and wind solutions and hypothesized that explosion occurs at the intersection between steady-state accretion solutions and steady-state wind solutions. By considering isothermal profiles, they were able to define an analytic condition that divides these solutions. For $c_T^2/v_{\text{esc}}^2 > 3/16$, only wind solutions are possible, which they attribute to the transition between steady-state accretion and explosion. Given the great deal of neutrino heating and neutrino cooling, the post-shock profile is certainly not isothermal. Therefore, they were unable to derive a similar analytic condition in a more realistic CCSN context. Instead, they solved the steady-state equations and empirically searched for a similar condition that would be appropriate for the core-collapse case. The resulting explosion condition that they propose is the antesononic condition, $\max(c_s^2/v_{\text{esc}})^2 \gtrsim 0.19$, where $\max()$ denotes the maximum in between the NS and the shock. Empirically, our 1D simulations indicate that a value of ~ 0.19 is about right. However, in multi-D simulations, Müller et al. (2012a) and Burrows (2013) found a much higher value of ~ 0.3 . If the antesononic is correct in spirit, it clearly is missing some important physics. To use the antesononic condition in practice, one must measure the “critical” condition in simulations *ex post facto*. The antesononic condition which is analytically derived in the isothermal case and empirically derived in the non-isothermal case is by no means perfect, but Figure 10 shows that it fares a little better than the timescale ratio condition.

While the antesononic conditions fair much better than the timescale ratio at predicting explosion, it still remains less favorable compared to the integral condition (middle panel of Figure 10). For one, like the timescale ratio, the dramatic upward trend in the antesononic feature which might be attributed to explosion actually occurs well after explosion; so one can rule out using the upward trend as an explosion diagnostic. One of the useful features of the integral condition, $\Psi_{\min} > 0$ is that one can tell even before explosion that a model is unlikely to explode. There are two features that enable this: 1) the closeness of Ψ_{\min} to zero, and 2) the trend toward or away from zero; for example, Ψ_{\min} for the $L_\nu = 3.0$ model marches toward explosion while Ψ_{\min} for the $L_\nu = 2.0$ model marches away from explosion. Similar to point 1) for the integral condition, the antesononic condition is indeed closer to the “critical” value before explosion. However, even the antesononic diagnostic for the $L_\nu = 2.0$ marches toward the “critical” value even though it never explodes. Furthermore, the antesononic diagnostic overshoots the “critical” value by $\sim 10\%$ of the “critical” value. This may seem like a triumph of estimating the “critical” value, but the dynamic range of the antesononic diagnostic is only $\sim 20\%$ of the “critical” value, making the estimate only $\sim 50\%$ accurate when considering the dynamic range of the antesononic diagnostic.

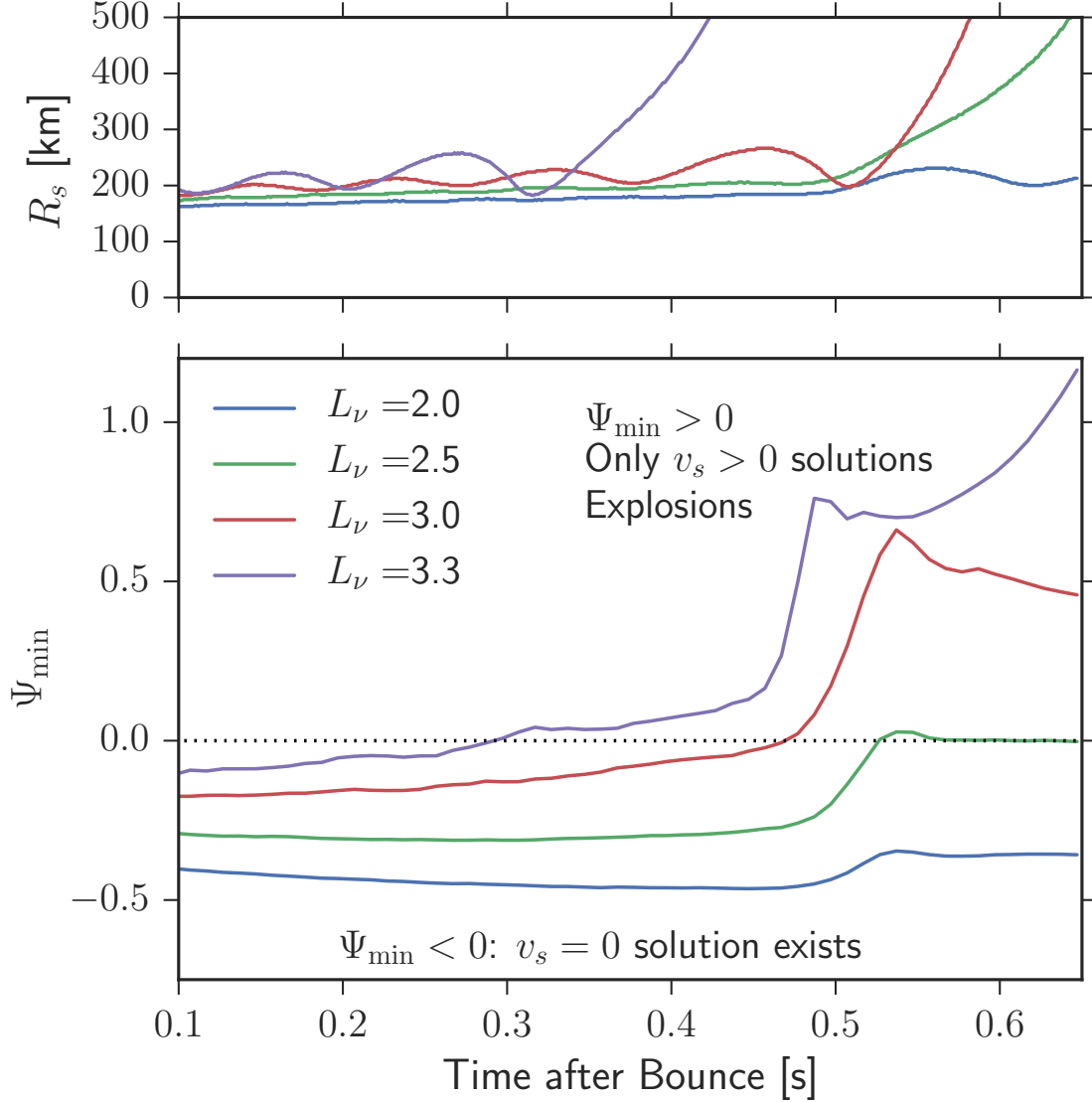


Figure 7. Nearness-to-explosion condition for 1D hydrodynamic simulations: Ψ_{\min} vs. time. For each time, we extract the important parameters of the problem (L_ν , T_ν , R_{NS} , M_{NS} , and \dot{M}) from the 1D hydrodynamic simulations and calculate the family of steady-state solutions. Ψ_{\min} represents the minimum possible value of Ψ over that family (See Figure 5). While $\Psi_{\min} < 0$, there exists a stalled accretion shock solution ($\Psi = 0$ and $v_s = 0$). When $\Psi_{\min} > 0$ all possible solutions have $v_s > 0$, which we associate with explosion. Empirically, we find that before explosion $\Psi_{\min} < 0$ and during explosion $\Psi_{\min} > 0$. Most importantly, the value of Ψ_{\min} offers an excellent indication of nearness to explosion.

7. DISCUSSION AND CONCLUSIONS

For many years, the critical neutrino luminosity curve has been the most impactful model for understanding successful explosion conditions. However, no one had demonstrated that the solutions above the curve are explosive, nor had anyone successfully used the critical neutrino luminosity as an explosion diagnostic for core-collapse simulations. In this manuscript, we do both. When we began this project, our primary goal was to merely show that the solutions above the critical neutrino luminosity curve are explosive. We have partially done so by deriving an integral condition, $\Psi_{\min} \geq 0$, for $v_s \geq 0$ and showing that the solutions above the critical neutrino luminosity curve have $v_s > 0$. Along the way to deriving this integral condition, we discovered that

the neutrino luminosity curve is a projection of a more general critical hypersurface. Most strikingly, that critical hypersurface is represented by a single dimensionless parameter, $\Psi_{\min} \geq 0$, and it promises to be a useful explosion diagnostic for core-collapse simulations.

In deriving the integral condition $\Psi \geq 0$, we make two simple but profound approximations: 1) we consider steady-state solutions and 2) $v_s > 0$ corresponds to explosion. With these two approximations, we derive an integral condition for $v_s \geq 0$ and recast it in a dimensionless form, $\Psi \geq 0$. We verify this integral condition using 1D parameterized simulations and find that during the stalled shock phase $\Psi \approx 0$ and during explosion $\Psi > 0$. Though the comparisons with simulations successfully verify the integral condition, they also demon-

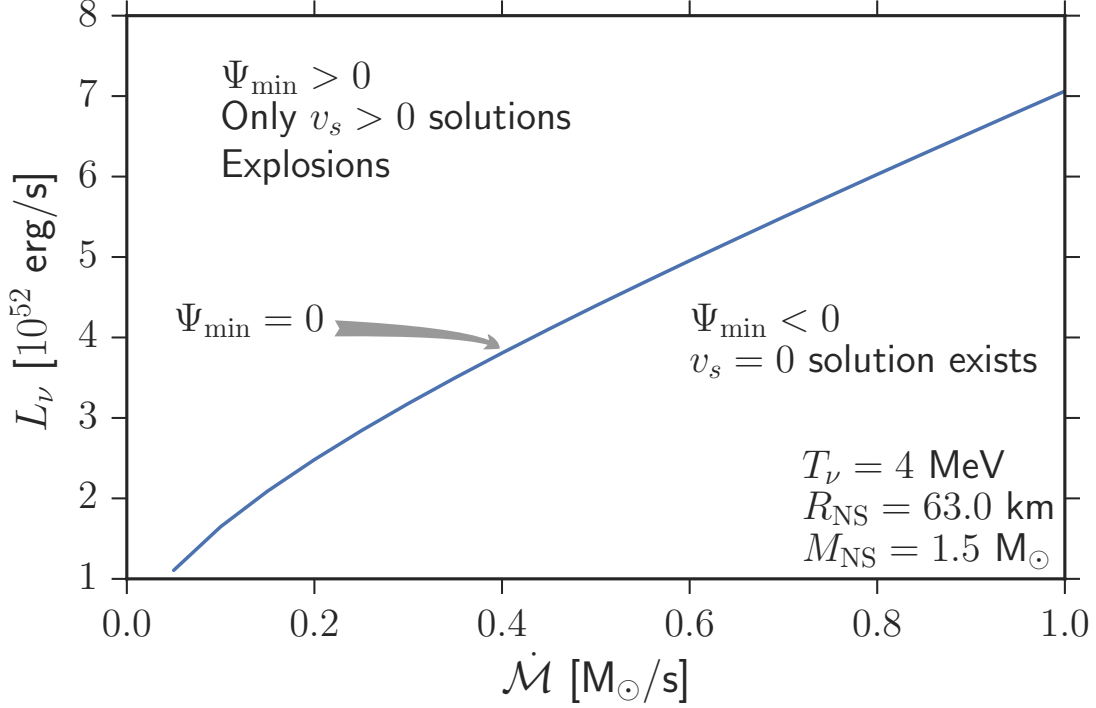


Figure 8. Here we use the $\Psi_{\min} > 0$ condition to derive the critical neutrino luminosity curve of Burrows & Goshy (1993) and show that the solutions above the critical neutrino luminosity for a given accretion rate have $v_s > 0$. To derive the critical neutrino luminosity, we fixed three of the five important parameters and restrict our exploration to the L_ν - \dot{M} plane. Then we find solutions to the steady-state equations and select the locus of solutions with $\Psi_{\min} = 0$. The resulting curve reproduces the critical neutrino luminosity. The solutions above this curve have $v_s > 0$ and below this curve, solutions with $v_s = 0$ exist. The critical neutrino luminosity curve is a projection of a more general critical hypersurface, and that critical hypersurface is represented by one dimensionless condition, $\Psi_{\min} = 0$.

strate that just calculating Ψ from the simulations is not a useful explosion diagnostic. Because the simulations always find a stalled shock solution before explosion, Ψ is always zero before explosion. Such a diagnostic fails to indicate a distance to explosion. If, on the other hand, we extract the important parameters from the simulations and calculate all of the possible steady-state solutions, a better diagnostic emerges.

The steady state solutions fall into one of two broad categories: in one category, a stalled-shock solution exists, and in the other, only $v_s > 0$ solutions exist. To understand the origin of these categories, one must first understand that there are five important parameters that characterize each steady-state solution: L_ν (neutrino luminosity), T_ν (neutrino temperature), R_{NS} (proto-neutron star radius), M_{NS} (proto-neutron star mass), and \dot{M} (accretion rate). For a fixed set of parameters, there are a family of solutions, and each solution in this family has a different value of Ψ . In general, Ψ may be negative, zero, or positive and because $\Psi \propto v_s$ each solution may have $v_s < 0$, $v_s = 0$, or $v_s > 0$. If a $v_s = 0$ solution exists, it represents the preferred quasi-equilibrium solution. Generically, for each family of solutions, there is a minimum Ψ which we denote Ψ_{\min} , and it is this parameter that determines whether a solution belongs to the stalled-shock category or the explosive category. If $\Psi_{\min} < 0$, then the family of solutions has solutions with $v_s < 0$, $v_s = 0$, and $v_s > 0$ with the $v_s = 0$ being the preferred quasi-equilibrium solution. If on the

other hand, $\Psi_{\min} > 0$, then only $v_s > 0$ solutions exist. If we attribute $v_s > 0$ to explosions, then Ψ_{\min} is a useful explosion diagnostic.

We calculate Ψ_{\min} for several 1D parameterized simulations (see Figure 7) and find that the time evolution of Ψ_{\min} makes an excellent explosion diagnostic. From the beginning of the simulation, one can tell if a simulation is near explosion or not. For those that are near explosion, Ψ_{\min} tends to march toward explosion throughout much of the simulation. The model that does not explode shows a general evolution of Ψ_{\min} away from explosion. In a forthcoming paper (Murphy & Dolence in prep. 2015), we plan to study Ψ_{\min} in self-consistent neutrino radiation hydrodynamics simulations to see if these promising behaviors remain.

In section 6 and Figures 9 & 10, we compare this new integral condition with explosion conditions that have been previously defined. Specifically, we compare $\Psi_{\min} > 0$ to a timescale ratio condition and the antesononic condition. In contrast to the integral condition, the $\tau_{\text{adv}}/\tau_{\text{heat}}$ condition is heuristic, only good to order unity, shows no obvious “critical” value, and is no better than just using R_s as an explosion diagnostic. The antesononic condition fares better than the timescale ratio condition. Even so, it lacks the accuracy and predictive attributes of the integral condition.

To derive the integral condition, we made two approximations that must be investigated further: we assume that $v_s > 0$ corresponds to explosion, and we assume

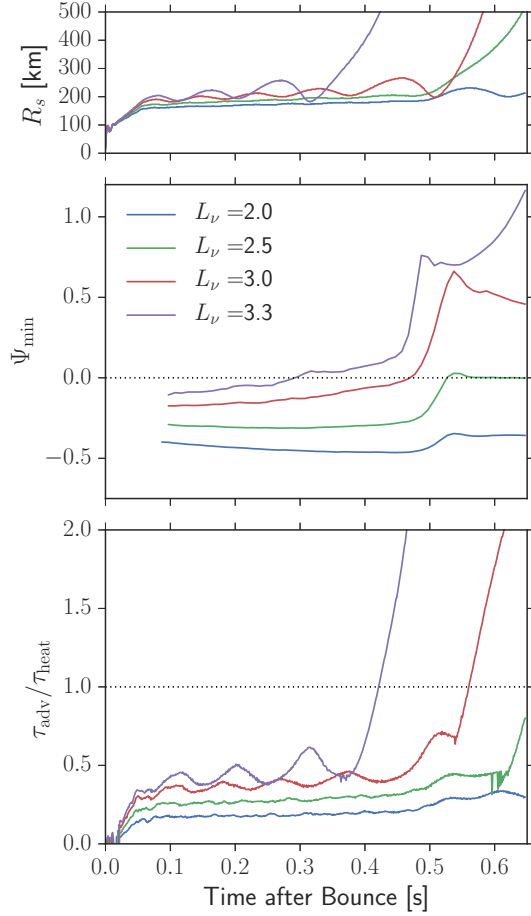


Figure 9. A comparison of the explosion diagnostic, $\Psi_{\min} > 0$, and a timescale ratio condition, $\tau_{\text{adv}}/\tau_{\text{heat}}$. The top plot shows Ψ_{\min} and the bottom plot shows the ratio of the advection time (τ_{adv}) to the heating time (τ_{heat}). The advection timescale is defined as $\tau_{\text{adv}} = M_{\text{gain}}/\dot{M}$, where M_{gain} is the mass in between the gain radius and the shock. We adopt a heating timescale that is a ratio of energy and heating rate in the gain region: $\tau_{\text{heat}} = E/Q_{\text{gain}}$, where $Q_{\text{gain}} = \int_{r_{\text{gain}}}^{R_s} (H - C)\rho dV$, and $E = \int_{\text{gain}} \epsilon \rho dV$ is the total internal energy in the gain region. The $\tau_{\text{adv}}/\tau_{\text{heat}}$ is an approximate heuristic explosion diagnostic. The choice of the terms to define the timescales and the region over which to integrate are arbitrary. The timescale ratio is $\mathcal{O}(1)$ but it shows no sign of a reliable “critical” value or utility in predicting explosion. In fact, it is only as good as using the shock radius as an explosion diagnostic. On the other hand, Ψ_{\min} works quite well as an explosion diagnostic.

steady-state throughout our derivation. These are two very strong assumptions that could have invalidated our derivation. For example, $v_s > 0$ does not necessarily equate to explosion, especially if we relax the steady-state condition. Oscillations of the shock are one example in which $v_s > 0$ may manifest but not lead to explosion. In order to make progress, we decided to see where these approximations lead. In the end, we were able to derive an integral explosion diagnostic that successfully describes the explosion conditions of parameterized 1D simulations. However, we do not show that once $\Psi_{\min} > 0$ and the shock begins to move outward that it continues to move outward. In some sense, one expects the shock to continue to move out, because once $\Psi_{\min} > 0$ the only steady-state solutions are ones with

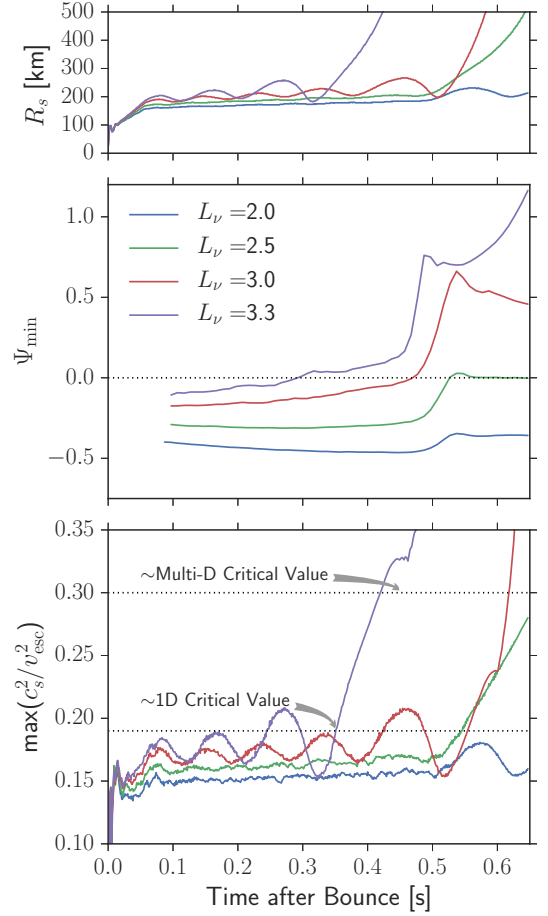


Figure 10. The Ψ_{\min} explosion diagnostic in comparison with the antesononic condition of Pejcha & Thompson (2012). For an isothermal flow in 1D, Pejcha & Thompson (2012) show that there are no steady-state accretion solutions that match the pre-shock flow for $c_s^2/v_{\text{esc}}^2 > 3/16$. By analogy, they propose that a similar condition exists for the non-isothermal situation of the core-collapse problem. By numerically exploring the steady-state solutions in 1D approximations, they propose that $\max(c_s^2/v_{\text{esc}}^2) \gtrsim 0.19$ divides steady-state accretion from explosion. In multi-D simulations, Müller et al. (2012a) and Dolence et al. (2013) empirically find that $\max(c_s^2/v_{\text{esc}}^2) \gtrsim 0.3$ is a better “critical” value. The bottom panel of this figure shows that the 1D “critical” value is a decent indicator of explosion. It certainly performs better than the timescale ratio seen in Figure 9. Still, the $\Psi_{\min} > 0$ condition has some practical advantages. For one, $\Psi_{\min} > 0$ is an integral condition derived from the supposition that $v_s > 0$ corresponds to explosion. Second, the dynamic range of Ψ_{\min} illustrates more clearly which simulations are far from explosion. Third, while the lowest luminosity model appears to always approach explosion for the $\max(c_s^2/v_{\text{esc}}^2)$ condition, the Ψ_{\min} condition clearly shows that the $L_\nu = 2.0$ model moves away from explosion, except when the density shell accretes through the shock, but then again it moves away from explosion. Fourth, $\max(c_s^2/v_{\text{esc}}^2) \gtrsim 0.19$ does not predict explosion: the actual antesononic condition overshoots the proposed critical value by 10% before it actually explodes, which is half of the full dynamic range of the antesononic condition ($\sim 20\%$); when the antesononic condition looks like it is indicating explosion, it does so well after the initiation of explosion.

$v_s > 0$, but this does not preclude the possibility of a dynamic (non steady-state) solution that is oscillatory. A next step in confirming our derivation is to show that once $\Psi_{\min} > 0$, the dynamic solution is one in which $v_s > 0$ continues.

We found the integral condition to be a successful ex-

plosion diagnostic for 1D parameterized explosions, but we suspect that it can do much more. We suspect that the integral condition may be an excellent explosion diagnostic for self-consistent 3D core-collapse supernova simulations. One may even be able to predict whether a certain progenitor model will explode without even performing core-collapse simulations. This hope will only be realized with further model developments, replacing parameters currently measured from simulations with parameters calculated by other means.

But before we can even pursue such bold endeavors, we must adapt the integral condition to include the appropriate physics. For one, we derive the integral condition using Newtonian gravity; general relativistic considerations are important, so we will need to take the straightforward steps in deriving the condition in GR. Second, we need to incorporate a more self-consistent neutrino heating and cooling. Third, we need to incorporate multi-dimensional effects. Turbulence seems to reduce the critical neutrino luminosity for explosion; we suspect that one can easily use a turbulence model to

derive a new integral condition for explosion including turbulence.

In summary, we derive an integral condition for explosion and verify it with 1D parameterized simulations. When combined with simple steady-state model's, it suggests a new explosion diagnostic, Ψ_{\min} , that we argue may be a more predictive measure of a models explosability than other diagnostics. Finally, we point out that our integral formulation can be extended with better physics, and we are hopeful that this approach may prove useful in disentangling the complicated interactions of various physical effects and in understanding the mechanism of core-collapse supernovae in Nature.

ACKNOWLEDGMENTS

We would like to acknowledge the pioneering work of Adam Burrows, Hans-Thomas Janka, and Mathias Liebendörfer whose contributions to CCSN theory were directly inspirational to the work presented here. This material is based upon work supported by the National Science Foundation under Grant No. 1313036.

APPENDIX

STEADY STATE EQUATIONS

Identifying the steady-state solution with the minimum Ψ is key in developing the explosion diagnostic in section 5 and Figure 7. Therefore, in this appendix, we present the steady-state equations and solution techniques that we used to obtain the family of solutions.

To accommodate the analytic EOS described in the next appendix, we recast the steady-state equations in terms of the natural independent variables. Because the analytic EOS in appendix B is most naturally written as a function of density and temperature, $P = P(\rho, T)$, we re-write the steady-state equations as differential equations for v , ρ , and T .

$$\frac{d \ln v}{d \ln r} = - \left(2 + \frac{d \ln \rho}{d \ln r} \right) \quad (\text{A1})$$

$$\frac{d \ln \rho}{d \ln r} \left(y P_\rho - \frac{v^2}{\phi} \right) = -y P_T \frac{d \ln T}{d \ln r} - 1 + \frac{2v^2}{\phi} \quad (\text{A2})$$

and

$$e_T \frac{d \ln T}{d \ln r} = (\gamma_4 - 1 - e_\rho) \frac{d \ln \rho}{d \ln r} - \frac{L_\nu \kappa \rho r}{\dot{M} \varepsilon} + \frac{\rho C_0 (T/T_0)^6}{\dot{M} \varepsilon}, \quad (\text{A3})$$

where $P_\rho = (\partial \ln P / \partial \ln \rho)_T$ is the partial derivative of P with respect to ρ at constant T . Equivalently, $P_T = (\partial \ln P / \partial \ln T)_\rho$, $e_\rho = (\partial \ln \varepsilon / \partial \ln \rho)_T$, and $e_T = (\partial \ln \varepsilon / \partial \ln T)_\rho$.

EQUATION OF STATE

For the 1D parameterized simulations, we use the tabulated EOS provided by Hempel et al. (2012). The microphysics includes a distribution of nuclei that satisfy nuclear statistical equilibrium; the individual components are, broadly, a dense nuclear component, ideal gas for the nucleons and isotopes, photon gas, and relativistic electrons and positrons with arbitrary degeneracy. You may find the tabulated EOS and driver at <http://www.stellarcollapse.org/equationofstate>.

For the steady-state solutions we use an analytic EOS that does remarkably well in reproducing the microphysics in the region between the neutrino sphere and the shock. Bethe (1990), Janka (2001), and Fernández & Thompson (2009) were useful guides in developing this analytic EOS. First, we assume nuclear statistical equilibrium for three species only: neutrons, protons, and α s; their respective mass fractions are X_n , X_p , and X_α . Conservation of baryonic mass implies

$$X_n + X_p + X_\alpha = 1, \quad (\text{B1})$$

and conservation of charge implies

$$X_p + \frac{1}{2} X_\alpha = Y_e \quad (\text{B2})$$

where Y_e is the number of electrons per baryon. In our steady-state solutions we simply set $Y_e = 0.5$. In NSE, the

Saha equation provides the remaining equation to find a solution for the abundance of these three species.

$$X_n^2 X_p^2 = \frac{1}{2} X_\alpha \left(\frac{m_p n_q}{\rho} \right)^3 \exp\left(\frac{-Q_\alpha}{k_B T}\right), \quad (\text{B3})$$

with

$$n_q = \left(\frac{m_p k_B T}{2\pi\hbar^2} \right)^{3/2}, \quad (\text{B4})$$

and $Q_\alpha = 28$ MeV is the binding energy of the α .

We construct the pressure and internal energy under the assumptions that the photons, positrons, and electrons are relativistic and the partial pressure due to the nucleons and α s is given by the ideal gas law. In addition, we consider the electrons and positrons with an arbitrary degeneracy $\eta = \mu_e/(k_B T)$. The expression for the degeneracy parameter is

$$\rho = \frac{m_u}{3\pi^2 Y_e} \left(\frac{k_B T}{\hbar c} \right)^3 \eta(\pi^2 + \eta^2). \quad (\text{B5})$$

Both the pressure and internal energy may be divided into partial pressures due to relativistic (R) particles and nonrelativistic (NR) particles

$$P = P_R + P_{NR}, \quad (\text{B6})$$

and

$$\varepsilon = \varepsilon_R + \varepsilon_{NR}. \quad (\text{B7})$$

The partial pressure due to the relativistic constituents is

$$P_R = \frac{1}{12} \frac{(k_B T)^4}{(\hbar c)^3} \left(\frac{11\pi^2}{15} + 2\eta^2 + \frac{\eta^4}{\pi^2} \right), \quad (\text{B8})$$

and the partial pressure due to the nonrelativistic constituents is

$$P_{NR} = \left(1 - \frac{3}{4} X_\alpha \right) \frac{\rho k_B T}{m_u}. \quad (\text{B9})$$

The resulting internal energy is

$$\varepsilon = 3 \frac{P}{\rho} - \frac{3}{2} \frac{P_{NR}}{\rho} + (1 - X_\alpha) \frac{Q_\alpha}{4}, \quad (\text{B10})$$

where the last term is there to account for the transfer of binding energy per nucleon from X_α to the gas.

REFERENCES

- Bethe, H. A. 1990, *Reviews of Modern Physics*, 62, 801
 Bethe, H. A., & Wilson, J. R. 1985, *ApJ*, 295, 14
 Buras, R., Janka, H.-T., Rampp, M., & Kifonidis, K. 2006a, *A&A*, 457, 281
 Buras, R., Rampp, M., Janka, H.-T., & Kifonidis, K. 2006b, *A&A*, 447, 1049
 Burrows, A. 2013, *Reviews of Modern Physics*, 85, 245
 Burrows, A., & Goshy, J. 1993, *ApJ*, 416, L75
 Colgate, S. A., & White, R. H. 1966, *ApJ*, 143, 626
 Couch, S. M. 2013, *ApJ*, 775, 35
 Dolence, J. C., Burrows, A., Murphy, J. W., & Nordhaus, J. 2013, *ApJ*, 765, 110
 Dolence, J. C., Burrows, A., & Zhang, W. 2015, *ApJ*, 800, 10
 Fernández, R. 2012, *ApJ*, 749, 142
 Fernández, R., & Thompson, C. 2009, *ApJ*, 703, 1464
 Fryer, C. L., Belczynski, K., Wiktorowicz, G., Dominik, M., Kalogera, V., & Holz, D. E. 2012, *ApJ*, 749, 91
 Hanke, F., Marek, A., Müller, B., & Janka, H.-T. 2012, *ApJ*, 755, 138
 Hanke, F., Müller, B., Wongwathanarat, A., Marek, A., & Janka, H.-T. 2013, *ApJ*, 770, 66
 Hempel, M., Fischer, T., Schaffner-Bielich, J., & Liebendörfer, M. 2012, *ApJ*, 748, 70
 Hillebrandt, W., & Mueller, E. 1981, *A&A*, 103, 147
 Janka, H.-T. 2001, *A&A*, 368, 527
 —. 2012, *Annual Review of Nuclear and Particle Science*, 62, 407
 Janka, H.-T., & Keil, W. 1998, in *Supernovae and cosmology*, ed. L. Labhardt, B. Binggeli, & R. Buser, 7
 Lentz, E. J., Bruenn, S. W., Hix, W. R., Mezzacappa, A., Messer, O. E. B., Endeve, E., Blondin, J. M., Harris, J. A., Marronetti, P., & Yakunin, K. N. 2015, *ArXiv e-prints*
 Mazurek, T. J. 1982, *ApJ*, 259, L13
 Mazurek, T. J., Cooperstein, J., & Kahana, S. 1982, in *NATO Advanced Science Institutes (ASI) Series C, Vol. 90, NATO Advanced Science Institutes (ASI) Series C*, ed. M. J. Rees & R. J. Stoneham, 71–77
 Müller, B., Janka, H.-T., & Heger, A. 2012a, *ApJ*, 761, 72
 Müller, B., Janka, H.-T., & Marek, A. 2012b, *ApJ*, 756, 84
 Murphy, J. W., & Bloor, E. in prep. 2015
 Murphy, J. W., & Burrows, A. 2008, *ApJ*, 688, 1159

- Murphy, J. W., & Dolence, J. C. in prep. 2015
- Murphy, J. W., Dolence, J. C., & Burrows, A. 2013, *ApJ*, 771, 52
- O'Connor, E., & Ott, C. D. 2011, *ApJ*, 730, 70
- Ohnishi, N., Kotake, K., & Yamada, S. 2006, *ApJ*, 641, 1018
- Ott, C. D., Burrows, A., Dessart, L., & Livne, E. 2008, *ApJ*, 685, 1069
- Pejcha, O., & Thompson, T. A. 2012, *ApJ*, 746, 106
- Suwa, Y., Yamada, S., Takiwaki, T., & Kotake, K. 2014, *ArXiv e-prints*
- Takiwaki, T., Kotake, K., & Suwa, Y. 2014, *ApJ*, 786, 83
- Thompson, C. 2000, *ApJ*, 534, 915
- Thompson, T. A., Quataert, E., & Burrows, A. 2005, *ApJ*, 620, 861
- Woosley, S. E., & Heger, A. 2007, *Phys. Rep.*, 442, 269
- Yamasaki, T., & Foglizzo, T. 2008, *ApJ*, 679, 607
- Yamasaki, T., & Yamada, S. 2005, *ApJ*, 623, 1000
- . 2006, *ApJ*, 650, 291